Soot Nanoparticles Promote Biotransformation, Oxidative Stress, and Inflammation in Murine Lungs

Rodney L. Rouse[£], Gleeson Murphy[*†], Marc J. Boudreaux[‡], Daniel B. Paulsen[§], and Arthur L. Penn[*]*

[*]Comparative Biomedical Sciences, School of Veterinary Medicine, Louisiana State University, Baton Rouge, LA 70803. [£] Present address: U. S. Food and Drug Administratio, CDER, OPS, OTR, Department of Applied Pharmacology Research, White Oak Campus, Silver Spring, MD 20993. [†] Present address: U.S. Army Veterinary Medical Corps, Analytical Toxicology Division, USAMRICD, Aberdeen, MD 21010-5400. [‡] Division of Biotechnology & Molecular Medicine (BioMMED), School of Veterinary Medicine, Louisiana State University, Baton Rouge, LA 70803. [§] Pathobiological Sciences, School of Veterinary Medicine, Louisiana State University, Baton Rouge, LA 70803.

Urban ambient pollution particles, especially those derived from industrial/combustion processes, are composed of a complex array of organic and inorganic components, often adsorbed to a carbonaceous core. Exposure to ambient particles of a variety of sizes has been associated with increased cardiopulmonary morbidity and mortality and elevation of pro-inflammatory cytokines *in vivo* and *in vitro* (1-7). Ultrafine particles ($PM_{0.1}$; aerodynamic diameter < 0.1 μm) and nanoparticles (aerodynamic diameter < 0.150 μm) have received little attention from regulatory agencies (8), but in numerous experimental settings have been found to elicit a range of toxicological effects (9, 10). The surface characteristics and crystalline structure of ambient particles can be major determinants of pulmonary inflammation and injury (11, 12). Individually or in concert, complex chemicals adsorbed to particles can promote disease processes. Residual oil fly ash (ROFA) containing transition metals induces pulmonary inflammatory infiltrate, edema, and hemorrhage (13). Diesel exhaust particles (DEPs) containing a variety of oxygen radical-generating quinones, polyaromatic hydrocarbons (PAHs), and metal species (14-16) produce pulmonary inflammatory cell infiltration and cytokine production (17-19). A body of *in vitro* and *in vivo* literature has characterized the effects of parent particles and their isolated constituents in humans, as well as in animals (20, 21).

In urban areas, combustion of gasoline, diesel fuels, and industrial organics (simple aliphatics and/or fossil fuels) contributes significantly to the ambient $PM_{2.5}$ fine (22) and ultrafine particulate fractions (22-23). Incomplete combustion of low molecular weight hydrocarbons, e.g. during flaring at refineries, is a real source of complex environmental particulate contamination. Petrochemical-derived particulates resulting, by accident or sabotage, from refinery or pipeline explosions and fires also represent a real hazard both in the United States and abroad. Radicals formed early in combustion interact to form PAHs, including some carcinogens, from less complex structures. PAHs aggregate into nanoparticles, which can extend into branched-chain structures (soots). We have previously characterized the product of incomplete combustion of 1,3-butadiene. This product, butadiene soot (BDS), is both a model mixture and a real-life example of PAH-laden, combustion-derived nanoparticles with potential for environmental contamination and for acute and/or chronic health effects (24). BDS is an organic-rich mixture of 30-50 nm carbonaceous particles to which hundreds of PAH species, including benzo(a)pyrene [B(a)P] and other carcinogens, are adsorbed (24, 25). Both, human bronchoepithelial cells and mouse alveolar macrophages display a distinct punctate blue, PAH-associated cytoplasmic fluorescence following exposure to BDS *in vitro*. The fluorescence localizes to cytoplasmic lipid droplets even as Phase I biotransformation enzymes are induced (26). We hypothesized that inhalation of PAH-containing BDS will result in activation of aryl hydrocarbon receptor (AhR)-associated genes, as is the case with other PAH-rich mixtures (DEPs, cigarette smoke), will cause oxidative stress, and will result in inflammatory changes

METHODS

BDS Exposures: Eighteen 6-week old female Balb/c mice were obtained from Jackson Laboratories (Stock 000651, Bar Harbor, ME). All procedures were IACUC approved and in accord with NIH *Guide for the Care and Use of Laboratory Animals* (27). Ten mice inhaled BDS mixed with HEPA-filtered air (5.0 mg/m^3,4 hr/day, 4 days) and eight inhaled only HEPA-filtered air. Six BDS-exposed mice and four control mice were euthanized and sampled immediately following the fourth day of exposure. The remaining four mice from each group were euthanized and sampled the following day.

Airway Hyperresponsiveness: We assessed airway hyperresponsiveness in unrestrained mice by whole body plethysmography (Buxco, Troy, NY) immediately following the final BDS exposure.

Bronchoalveolar lavage fluid (BALF) Collection and Analysis: We lavaged lungs with phosphate-buffered saline. Leukocytes were categorized by type (macrophage, neutrophil, eosinophil) and macrophages were further graded by particle burden. Group 1 macrophages (MΦ1) had <10% cytoplasmic particle burden. Group 2 macrophages (MΦ2) had 10-50% of the cytoplasm occupied by particles. Group 3 macrophages (MΦ3) had > 50% of their cytoplasm occupied by particles. BALF was analyzed by enzyme-linked immunosorbent assay (ELISA; BD-Pharmingen, San Diego, C) for TNFα, IL-6, and Cxcl2.

Histopathology: The right lung was excised and stored in 0.02 M periodate-0.1 M lysine-0.25% paraformaldehyde (PLP) fixative prior to standard histological sectioning, staining, and evaluation. Histopathology was scored according to 6 parameters; particles found within 1) alveolar macrophages, 2) interstitial macrophages, and 3) bronchial epithelium; numbers of 4) peribronchial neutrophils, and 5) transmigratory neutrophils; and by 6) epithelial damage. Scoring was 0/1 (present or absent) for particulate matter in macrophages and epithelium. All other parameters were scored 0-3 (0, none; 1, mild; 2, moderate; 3, severe).

RNA Isolation: The left lung was stored in RNAlater (Applied Biosystems, Foster City, CA). Total RNA was extracted in TRIzol Reagent (Invitrogen, Carlsbad, CA).

Gene Microarray Assay: Global gene expression was assessed from total RNA on Mouse Genome 430 2.0 Arrays (Affymetrix, Santa Clara, CA). All data collected and analyzed here adhere to the guidelines for Minimal Information About a Microarray Experiment (MIAME).

Gene Expression Analysis: Expression Analysis Systems (Durham, NC) eliminated data from poor performing probe sets (REDI). Principle component analysis was used to determine clustering of experimental units. Treatment group data underwent permutation analysis for differential expression (PADE); including a false discovery rate (FDR) based on a permutation-generated reference curve (technical information on REDI and PADE analyses available at www.expressionanalysis.com). All transcripts included in this study had a fold change of at least 1.5 (up or down), and both an individual p-value and FDR ≤0.05.

Pathway Analysis: We analyzed gene expression data with the network- and pathway-building software, Ingenuity Pathways Analysis 4.0 and examined gene networks and canonical pathways using the Ingenuity Analysis Knowledge Database (Ingenuity Systems, Redwood City, CA).

Quantitative Real Time RT-PCR: We performed quantitative RT-PCR (qRT-PCR) for selected genes on cDNA from lung homogenates with inventoried TaqMan Gene Expression Assays primer-probe sets (Applied Biosystems, Foster City, CA).

Statistical Analysis: We used the UNIVARIATE and TTEST procedures of the SAS statistical package (version 9.1.3; SAS Institute, Inc., Cary, NC) to compare qRT-PCR data from lungs. We used SigmaStat 3.1 software (Systat Software Inc., San Jose, CA) to analyze cytokine data.

RESULTS

Airway Hyperresponsiveness: No significant differences between BDS-exposed mice and controls were noted with unrestrained whole body plethysmography (data not presented).

BALF Cytokines: IL-8 was significantly higher in BDS-exposed mice (data not presented). Following a day of recovery, IL-8 was further elevated in BDS-exposed mice. This finding is consistent with the increased BALF neutrophilia (described below) in these mice. No significant differences were detected in TNFα and IL-6 levels between BDS-exposed and control mice.

BALF Differentials: The differential cytology of BALF from air- and BDS-exposed mice, as well as the grouping of macrophages by particle burden, is presented in Figure 1.

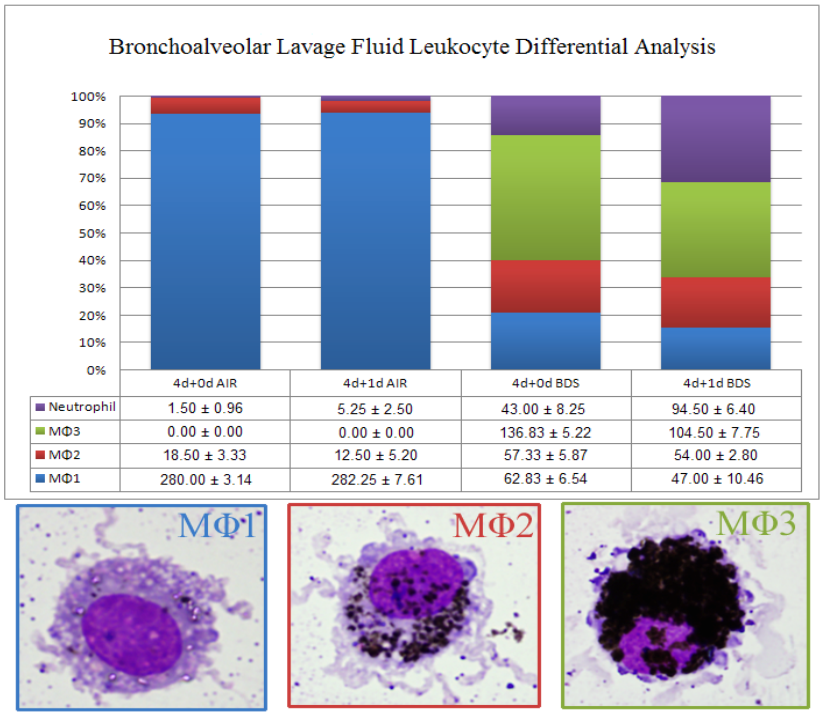

Figure 1: Differential Leukocyte Counts of BALF from Mice Exposed to Filtered Air or BDS. **In air control mice, essentially all the BALF cells were MΦ1 macrophages with fewer than five particles per cell. The source of those particles is unknown. In the BDS-exposed mice, neutrophil concentration was profoundly increased (>10X); < 1% of neutrophils contained particles. The particle burden of alveolar macrophages also was increased (> 50% of the macrophages present were Mϕ2 or Mϕ3); with one day recovery after BDS exposure, BALF neutrophilia increased in BDS-exposed mice (>2X; p=0.002).**

Lung Histopathology: Figure 2 shows histopathological changes in the lungs of control mice (2A), BDS-exposed mice sacrificed immediately after their final BDS exposure (2B), and BDS-exposed mice sacrificed one day following final exposure (2C). An inflammatory response in BDS-exposed mice sacrificed immediate after final exposure (2B) was evidenced by peribronchial neutrophilia and migration of neutrophils into the bronchoalveolar space. BDS-exposed mice sacrificed one day post-exposure, exhibited increasing neutrophilia, bronchiolar epithelial damage, including basement membrane disruption accompanied by the neutrophilic infiltration (Figure 2C). The BALF and histopathology results indicate that inhalation of these combustion-derived nanoparticles elicits a time-dependent increase in particle accumulation by alveolar macrophages, an associated deep lung neutrophilia, and persistence of particles in the pulmonary interstitium.

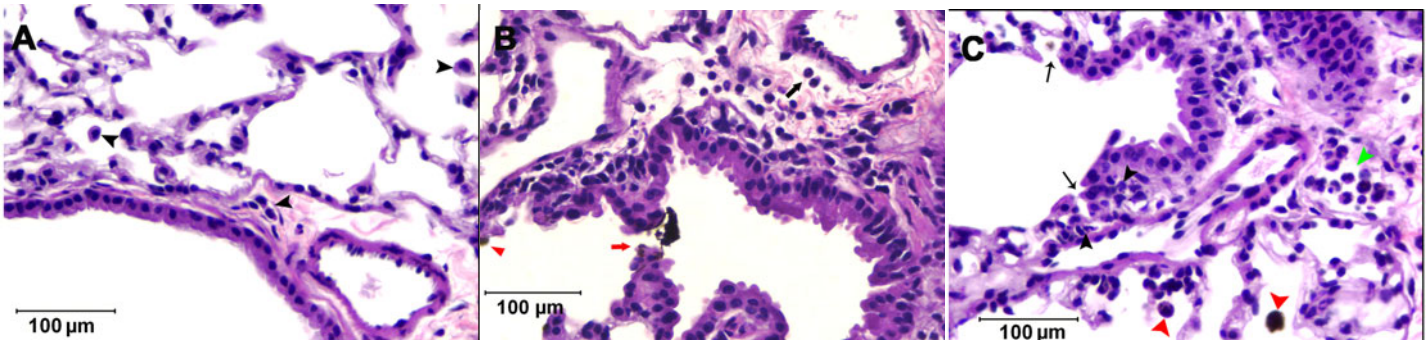

Figure 2: BDS-exposed mice experience a neutrophilic inflammatory pulmonary infiltrate.
A: Photomicrograph of a lung from a mouse exposed to HEPA-filtered air. Notice the scattered resident population of macrophages, in the interstitium and alveolar spaces (black arrowheads). H&E stain.
B. Photomicrograph of a lung from a mouse exposed to 5mg/m3 of BDS for 4 consecutive days and sacrificed immediately. Soot particles are within macrophages (red arrowhead) and bronchiolar epithelial cells (red arrow). Neutrophils are migrating into the bronchiolar interstitium (black arrows) but not through the epithelium. H&E stain.
C: Photomicrograph of a lung from a mouse exposed to 5 mg/m3 of BDS for four consecutive days then allowed rest for one day. Soot particles are within alveolar (red arrowheads) and interstitial macrophages. There is a focus of moderate neutrophilic infiltration and transmucosal exocytosis (black arrowheads) with mild disruption of the continuity of the bronchiolar epithelium (black arrows). An interstitial lymphatic vessel is filled with neutrophils (green arrowhead), most of which contain 1-3 individual soot particles (not apparent at this magnification). H&E stain.

Microarray: A total of 261 transcripts (73 down-regulated and 188 up-regulated) passed all criteria (≥ 1.5 fold-change, $p \leq 0.05$, FDR ≤ 0.05) in mice sacrificed immediately following 4 days of BDS exposure. Ingenuity Systems identified 248 of these transcripts as154 unique genes (33 down-regulated and 121 up-regulated). Aryl hydrocarbon receptor (Ahr)-related genes, oxidative stress response genes, and genes associated with inflammation were up-regulated (Table 1).

Quantitative RT-PCR: We performed qRT-PCR on lung tissue to confirm that BDS inhalation elicited up-regulation of biotransformation enzyme and inflammatory cytokine genes (Table 2). In the lungs of mice sacrificed immediately after BDS exposure, significant increases in expression were confirmed for selected AhR-responsive biotransformation enzymes. Chemokine (C-X-C motif) ligand 2 (Cxcl2; MIP-2; human IL-8 analog) up-regulation was confirmed by qRT-PCR. Il6 up-regulation was demonstrated by qRT-PCR but was not seen on microarray, a phenomenon that we have previously reported for other BALF-derived interleukins (28).

DISCUSSION

We have demonstrated that inhalation of combustion-derived BDS nanoparticles causes acute pulmonary inflammation in the bronchoalveolar space of mice. Metals-rich ROFA, oxygen-rich DEPs, and tobacco smoke particles also produce inflammatory lung infiltrate. Effects of these combustion products have been attributed to metals (13) hydroquinones oxidized to semiquinone radicals that ultimately produce superoxide (29) and other PAH oxidation products. Although oxidation of PAHs in BDS clearly occurs within the cell (Tables 1 & 2), the low oxygen content of BDS indicates that, unlike DEP and cigarette smoke, the initial chemical presentation of BDS to the cell is not primarily in the form of quinones, hydroquinones, and semiquinones. The numerous PAHs, including extensively investigated carcinogens, e.g., B(a)P, found in DEPs and cigarette smoke are metabolized for

detoxification and excretion (30, 31). The first step in this process is Phase I biotransformation. Our results reveal up-regulation of Phase I biotransformation genes in response to BDS inhalation.

The oxidized products of select PAHs metabolized by the cytochrome P450 system are capable of forming carcinogenic DNA adducts and/or eliciting oxidative stress responses in cells (32). These effects may be exacerbated by the presence of particles, as in the case of DEPs, where cellular oxidative stress

Table 1: Up-Regulated AhR, Oxidative Stress, and Inflammatory Genes in Lungs of BDS-Exposed Mice

Fold Change (versus Control)	Affymetrix ID	Name	Description
AhR			
5.913	1420796_at	AHRR	aryl-hydrocarbon receptor repressor
8.272	1418752_at	ALDH3A1	aldehyde dehydrogenase 3 family, memberA1
1.917	1417910_at	CCNA2	cyclin A2
15.919	1422217_a_at	CYP1A1	cytochrome P450, family 1, subfamily A, polypeptide 1
64.77	1416613_at	CYP1B1	cytochrome P450, family 1, subfamily B, polypeptide 1
1.506	1423828_at	FASN	fatty acid synthase
2.432	1452160_at	TIPARP	TCDD-inducible poly(ADP-ribose) polymerase
Oxidative Stress			
1.685	1423100_at	FOS	v-fos FBJ murine osteosarcoma viral oncogene homolog
1.823	1455959_s_at	GCLC	glutamate-cysteine ligase, catalytic subunit
1.585	1449279_at	GPX2	glutathione peroxidase 2 (gastrointestinal)
1.603	1448239_at	HMOX1	heme oxygenase (decycling) 1
1.523	1416543_at	NFE2L2	nuclear factor (erythroid-derived 2)-like 2
6.139	1423627_at	NQO1	NAD(P)H dehydrogenase, quinone 1
1.582	1421529_a_at	TXNRD1	thioredoxin reductase 1
Inflammatory/Immune			
2.152	1418133_at	BCL3	B-cell CLL/lymphoma 3
3.407	1422029_at	CCL20	chemokine (C-C motif) ligand 20
2.564	1455577_at	CCL28	chemokine (C-C motif) ligand 28
1.529	1423466_at	CCR7	chemokine (C-C motif) receptor 7
2.294	1417268_at	CD14	CD14 molecule
10.433	1419209_at	CXCL2	chemokine (C-X-C motif) ligand 2
1.722	1449984_at	CXCL3	chemokine (C-X-C motif) ligand 3
2.619	1419728_at	CXCL6	chemokine (C-X-C motif) ligand 6 (granulocyte chemotactic protein 2)
1.71	1421034_a_at	IL4R	interleukin 4 receptor
1.612	1417483_at	NFKBIZ	nuclear factor of kappa light polypeptide gene enhancer in B-cells inhibitor, zeta
5.191	1417262_at	PTGS2	prostaglandin-endoperoxide synthase 2 (prostaglandin G/H synthase and cyclooxygenase)
2.195	1455899_x_at	SOCS3	suppressor of cytokine signaling 3

All gene symbols presented are for the human homolog. These data are from female mice that were sacrificed immediately following final BDS exposure; n = 4 in both groups. Individual microarrays were analyzed for each mouse (non-pooled samples). Gene expression changes were considered significant only if they passed all filtering criteria ($p \leq 0.05$, FDR ≤ 0.05, fold-change ≥ 1.5).

Table 2: Quantitative RT-PCR of lung tissue reveals up-regulation of aryl hydrocarbon receptor responsive biotransformation and inflammatory cytokine genes following inhalation exposure to BDS

Gene Abbreviation	Applied Biosystems Primer-Probe Set ID Number	4d+0d	4d+1d
AhR-Responsive Genes			
Ahr	Mm00478932_m1	-1.03 ± 0.16	1.00 ± 0.20
Ahrr	Mm00477443_m1	59.93 ± 8.95**	5.97 ± 1.22**
Aldh3a1	Mm00839312_m1	7.37 ± 1.05**	1.31 ± 0.28
Cyp1a1	Mm00487218_m1	35.87 ± 4.27**†	11.61 ± 2.44**
Cyp1b1	Mm00487229_m1	67.99 ± 9.83**	9.74 ± 2.11**
Tiparp	Mm00724822_m1	1.90 ± 0.28**	-1.19 ± 0.16
Cytokines			
Cxcl2 (MIP-2; IL-8)	Mm00436450_m1	7.82 ± 1.08**	4.94 ± 0.91**
Ifng	Mm00801778_m1	-1.37 ± 0.13	1.14 ± 0.30
Il-1b	Mm00434228_m1	1.22 ± 0.25	1.91 ± 0.44*
Il-4	Mm00445259_m1	-1.20 ± 0.14	1.07 ± 0.19†
Il-6	Mm00446190_m1	5.51 ± 1.30**	3.17 ± 0.72*
Tgfb1	Mm00441724_m1	1.01 ± 0.11	1.02 ± 0.15
Tnf	Mm00443258_m1	1.50 ± 0.24	1.63 ± 0.45

Results are reported as fold change over control ± standard error of the mean [($2^{-\Delta\Delta CT}$) ± SEM].
***significance p<0.05; **significance p<0.0001; †Unequal variance among samples; therefore, Satterthwaite's approximation was used for degrees of freedom in determining significance.**

has been linked directly to inflammatory endpoints (17). We have demonstrated up-regulation both of Nrf2 oxidative stress response genes and of pro-inflammatory genes in the lungs of mice following BDS exposure. NRF2 induces expression of HMOX1, NQO1, GPX2, and TXNRD1 in human tissues (33). Here, expression of Nfe2l2 (mouse homolog of NRF2) induces each of these genes in the lungs BDS-exposed mice. With increasing oxidative stress, inflammatory responses also escalate. In support of this, we demonstrate oxidative stress responses and inflammatory responses in the lungs of mice that have inhaled BDS.

Up-regulation of Il6, Cxcl2 (mouse homolog of IL8), Cxcl3, and Cxcl6 can lead to recruitment of neutrophils and macrophages to the lungs and is consistent with the neutrophilic inflammatory response observed histopathologically in lung sections. These inflammatory effectors may be produced by pulmonary epithelial cells (34) or fibroblasts (35). A significant influx of neutrophils to the bronchoalveolar space also was observed via BALF cytology. Consistent with the neutrophilia, BALF IL-8 levels were elevated in BDS-exposed mice. Increasing neutrophilia was accompanied by the emergence of MΦ2s and MΦ3s in the BALF and pulmonary interstitium (Figure 2C).

Inhalation of particles may elicit not only local effects in the respiratory tract, but systemic effects, as well. An increase in circulating levels of inflammatory cytokines subsequent to PM_{10} exposure has been associated with progression of atherosclerosis (36). Direct translocation of particle*s* from the

respiratory tree to the systemic circulation has been described as influencing the subsequent development of cardiovascular disease conditions (37), although this conclusion has been actively challenged by more recent human exposure studies (38, 39). Ultrafine particles deposited in the nasopharyngeal area access the central nervous system via olfactory neuronal transport (40). Studies in rats and dogs have demonstrated that pulmonary epithelial cells have a saturation point with respect to PAHs (41). Combustion-derived ultrafine particles have the potential to translocate to extrapulmonary sites *with* their PAH payload intact, if this PAH saturation point is exceeded. This is unlikely through exposure to ambient environmental particles which usually are present in relatively low concentration and have a low overall PAH burden (42). The saturating concentration might be exceeded however, during an acute exposure to high levels of such particles among firefighters, rescue workers, and local residents following a terrorist attack (as in September 11th), petrochemical industrial accidents, or soldiers and civilian populations exposed to petroleum fires (as in the Gulf Wars).

In summary, we have reported that brief inhalation exposure to a moderate dose of PAH-rich, metals-poor combustion-derived ultrafine BDS particles initiates 1) AhR-responsive biotransformation responses capable of transforming PAHs into more toxic metabolites, as evidenced by increased expression of AhR-responsive genes; 2) cellular oxidative stress, as reflected by up-regulation of Nrf2-mediated oxidative stress response genes and 3) acute pulmonary inflammation, as demonstrated by inflammatory cell infiltration and up-regulation of pro-inflammatory cytokine genes. Finally, our histopathological analyses indicate that freshly-generated inhaled BDS nanoparticles reach the deepest bronchoalveolar spaces in lungs of exposed mice.

References

1. Schwartz J, Dockery DW, Neas LM. Is daily mortality associated specifically with fine particles? *J Air Waste Manag Assoc* 1996; 46(10):927-939.
2. Pope CA, 3rd, Burnett RT, Thun MJ, Calle EE, Krewski D, Ito K, Thurston GD. Lung cancer, cardiopulmonary mortality, and long-term exposure to fine particulate air pollution. *JAMA* 2002; 287(9):1132-1141.
3. Pope CA, 3rd, Burnett RT, Thurston GD, Thun MJ, Calle EE, Krewski D, Godleski JJ. Cardiovascular mortality and long-term exposure to particulate air pollution: Epidemiological evidence of general pathophysiological pathways of disease. *Circulation* 2004; 109(1):71-77.
4. Dominici F, Peng RD, Bell ML, Pham L, McDermott A, Zeger SL, Samet JM. Fine particulate air pollution and hospital admission for cardiovascular and respiratory diseases. *JAMA* 2006; 295(10):1127-1134.
5. Kunzli N, Kaiser R, Medina S, Studnicka M, Chanel O, Filliger P, Herry M, Horak F, Jr., Puybonnieux-Texier V, Quenel P, Schneider J, Seethaler R, Vergnaud J C, Sommer H.
Public-health impact of outdoor and traffic-related air pollution: A European assessment. *Lancet* 2000; 356(9232):795-801.
6. van Eeden SF, Tan WC, Suwa T, Mukae H, Terashima T, Fujii T, Qui D, Vincent R, Hogg JC. Cytokines involved in the systemic inflammatory response induced by exposure to particulate matter air pollutants (pm(10)). *Am J Respir Crit Care Med* 2001; 164(5):826-830.
7. Fujii T, Hayashi S, Hogg JC, Vincent R, Van Eeden SF. Particulate matter induces cytokine expression in human bronchial epithelial cells. *Am J Respir Cell Mol Biol* 2001; 25(3):265-271.
8. United States Environmental Protection Agency. National ambient air quality standards for particulate matter. Standards for particulate matter.: Federal Registry 1997 62(3): 138.

9. Bermudez E, Mangum JB, Wong BA, Asgharian B, Hext PM, Warheit DB, Everitt JI. Pulmonary responses of mice, rats, and hamsters to subchronic inhalation of ultrafine titanium dioxide particles. *Toxicol Sci* 2004; 77(2):347-357.
10. Lundborg M, Dahlen SE, Johard U, Gerde P, Jarstrand C, Camner P, Lastbom L. Aggregates of ultrafine particles impair phagocytosis of microorganisms by human alveolar macrophages. *Environ Res* 2006; 100(2):197-204.
11. Sayes CM, Reed KL, Warheit DB. Assessing toxicity of fine and nanoparticles: Comparing in vitro measurements to in vivo pulmonary toxicity profiles. *Toxicol Sci* 2007; 97(1):163-180.
12. Warheit DB, Webb TR, Colvin VL, Reed KL, Sayes CM. Pulmonary bioassay studies with nanoscale and fine-quartz particles in rats: Toxicity is not dependent upon particle size but on surface characteristics. *Toxicol Sci* 2007; 95(1):270-280.
13. Dreher KL, Jaskot RH, Lehmann JR, Richards JH, McGee JK, Ghio AJ, Costa DL. Soluble transition metals mediate residual oil fly ash induced acute lung injury. *J Toxicol Environ Health* 1997; 50(3):285-305.
14. Kumagai Y, Koide S, Taguchi K, Endo A, Nakai Y, Yoshikawa T, Shimojo N. Oxidation of proximal protein sulfhydryls by phenanthraquinone, a component of diesel exhaust particles. *Chem Res Toxicol* 2002; 15(4):483-489.
15. Li N, Venkatesan MI, Miguel A, Kaplan R, Gujuluva C, Alam J, Nel A. Induction of heme oxygenase-1 expression in macrophages by diesel exhaust particle chemicals and quinones via the antioxidant-responsive element. *J Immunol* 2000; 165(6):3393-3401.
16. Murphy SA, BeruBe KA, Richards RJ. Bioreactivity of carbon black and diesel exhaust particles to primary clara and type ii epithelial cell cultures. *Occup Environ Med* 1999; 56(12):813-819.
17. Ma JY, Ma JK. The dual effect of the particulate and organic components of diesel exhaust particles on the alteration of pulmonary immune/inflammatory responses and metabolic enzymes. *J Environ Sci Health C Environ Carcinog Ecotoxicol Rev* 2002; 20(2):117-147.
18. Rao KM, Ma JY, Meighan T, Barger MW, Pack D, Vallyathan V. Time course of gene expression of inflammatory mediators in rat lung after diesel exhaust particle exposure. *Environ Health Perspect* 2005; 113(5):612-617.
19. Saber AT, Jacobsen NR, Bornholdt J, Kjaer SL, Dybdahl M, Risom L, Loft S, Vogel U, Wallin H. Cytokine expression in mice exposed to diesel exhaust particles by inhalation. Role of tumor necrosis factor. *Part Fibre Toxicol* 2006; 3:4.
20. Diaz-Sanchez D, Tsien A, Fleming J, Saxon A. Combined diesel exhaust particulate and ragweed allergen challenge markedly enhances human in vivo nasal ragweed-specific IgE and skews cytokine production to a T helper cell 2-type pattern. *J Immunol* 1997; 158(5):2406-2413.
21. Salvi S, Blomberg A, Rudell B, Kelly F, Sandstrom T, Holgate ST, Frew A. Acute inflammatory responses in the airways and peripheral blood after short-term exposure to diesel exhaust in healthy human volunteers. *Am J Respir Crit Care Med* 1999; 159(3):702-709.
22. Lighty JS, Veranth JM, Sarofim AF. Combustion aerosols: Factors governing their size and composition and implications to human health. *J Air Waste Manag Assoc* 2000; 50(9):1565-1618; discussion 1619-1522.
23. Oberdorster G, Ferin J, Lehnert BE. Correlation between particle size, *in vivo* particle persistence, and lung injury. *Environ Health Perspect* 1994; 102 Suppl 5:173-179.
24. Penn A, Murphy G, Barker S, Henk W, Penn L. Combustion-derived ultrafine particles transport organic toxicants to target respiratory cells. *Environ Health Perspect* 2005; 113(8):956-963.
25. Catallo WJ, Kennedy CH, Henk W, Barker SA, Grace SC, Penn A. Combustion products of 1,3-butadiene are cytotoxic and genotoxic to human bronchial epithelial cells. *Environ Health Perspect* 2001; 109(9):965-971.
26. Murphy G, Rouse R, Polk W, Henk W, Barker S, Boudreaux M, Floyd Z, Penn A. Combustion-derived hydrocarbons localize to respiratory cell lipid droplets and up-regulate biotransformation enzymes. *Am J Respir Cell Mol Biol* 2008; (in press).
27. Institute of Laboratory Animal Resources. Guide for the care and use of laboratory animals. . Washington, DC: National Academy Press; 1996.
28. Rouse RL, Boudreaux MJ, Penn AL. In utero environmental tobacco smoke exposure alters gene expression in lungs of adult BALB/c mice. *Environ Health Perspect* 2007; 115(12):1757-1766.
29. Pryor WA. Cigarette smoke radicals and the role of free radicals in chemical carcinogenicity. *Environ Health Perspect* 1997; 105 Suppl 4:875-882.
30. Bonvallot V, Baeza-Squiban A, Baulig A, Brulant S, Boland S, Muzeau F, Barouki R, Marano F. Organic compounds from diesel exhaust particles elicit a proinflammatory response in human airway epithelial cells and induce cytochrome p450 1a1 expression. *Am J Respir Cell Mol Biol* 2001; 25(4):515-521.
31. Kim JY, Hecht SS, Mukherjee S, Carmella SG, Rodrigues EG, Christiani DC. A urinary metabolite of phenanthrene as a biomarker of polycyclic aromatic hydrocarbon metabolic activation in workers exposed to residual oil fly ash. *Cancer Epidemiol Biomarkers Prev* 2005; 14(3):687-692.

32. Connery A. Induction of microsomal enzymes by foreign chemicals and carcinogenesis by polycyclic aromatic hydrocarbons. *Cancer Res* 1982; 42: 4875-4917.
33. Yamamoto J, Ihara K, Nakayama H, Hikino S, Satoh K, Kubo N, Iida T, Fujii Y, Hara T. Characteristic expression of aryl hydrocarbon receptor repressor gene in human tissues: Organ-specific distribution and variable induction patterns in mononuclear cells. *Life Sci* 2004; 74(8):1039-1049.
34. Masubuchi T, Koyama S, Sato E, Takamizawa A, Kubo K, Sekiguchi M, Nagai S, Izumi T. Smoke extract stimulates lung epithelial cells to release neutrophil and monocyte chemotactic activity. *Am J Pathol* 1998; 153(6):1903-1912.
35. Sato E, Koyama S, Takamizawa A, Masubuchi T, Kubo K, Robbins RA, Nagai S, Izumi T. Smoke extract stimulates lung fibroblasts to release neutrophil and monocyte chemotactic activities. *Am J Physiol* 1999; 277(6 Pt 1):L1149-1157.
36. Suwa T, Hogg JC, Quinlan KB, Ohgami A, Vincent R, van Eeden SF. Particulate air pollution induces progression of atherosclerosis. *J Am Coll Cardiol* 2002; 39(6):935-942.
37. Nemmar A, Hoylaerts MF, Hoet PH, Nemery B. Possible mechanisms of the cardiovascular effects of inhaled particles: Systemic translocation and prothrombotic effects. *Toxicol Lett* 2004; 149(1-3):243-253.
38. Mills NL, Amin N, Robinson SD, Anand A, Davies J, Patel D, de la Fuente JM, Cassee FR, Boon NA, Macnee W, Millar A M, Donaldson K, Newby D E. Do inhaled carbon nanoparticles translocate directly into the circulation in humans? *Am J Respir Crit Care Med* 2006; 173(4):426-431.
39. Wiebert P, Sanchez-Crespo A, Seitz J, Falk R, Philipson K, Kreyling WG, Moller W, Sommerer K, Larsson S, Svartengren M. Negligible clearance of ultrafine particles retained in healthy and affected human lungs. *Eur Respir J* 2006; 28(2):286-290.
40. Elder A, Gelein R, Silva V, Feikert T, Opanashuk L, Carter J, Potter R, Maynard A, Ito Y, Finkelstein J, Oberdorster G. Translocation of inhaled ultrafine manganese oxide particles to the central nervous system. *Environ Health Perspect* 2006; 14(8):1172-1178.
41. Ewing P, Blomgren B, Ryrfeldt A, Gerde P. Increasing exposure levels cause an abrupt change in the absorption and metabolism of acutely inhaled benzo(a)pyrene in the isolated, ventilated, and perfused lung of the rat. *Toxicol Sci* 2006; 91(2):332-340.
42. Allen J, Dookeran KM, Smith KA, Sarofim AF, Taghizadeh K, Lafleur AL. Measurement of polycyclic aromatic hydrocarbons associated with size-segregated atmospheric aerosols in Massachusetts. *Environ Sci & Tech* 1996; 30(3):1023-1031